Pyrazolate-Based Dinucleating Ligands in L_2M_2 Scaffolds: Effects of Bulky Substituents and Coligands on Structures and M···H−C Interactions

Jens C. Röder,[b][‡] Franc Meyer,*[a] Elisabeth Kaifer,[b] and Hans Pritzkow[b]

Keywords: Nickel / Palladium / Dinuclear complexes / N-ligands / Pyrazole ligands

A series of nickel(II) and palladium(II) complexes $[L_2M_2]^{2+}$ have been prepared and structurally characterized, where L is a pyrazolate ligand with bulky 2,6-dimethyl- or 2,6-di(isopropyl)anilinomethyl side arms. Coordinating counter anions such as chloride can bind to axial sites of the dinickel species in a solvent-dependent process, giving rise to five-coordinate high-spin metal ions. In the case of weakly coordinating anions, the metal ions are found in roughly square-planar environments, and the structures are governed by the tendency of the bulky aryl groups to avoid each other, which forces the methyl or isopropyl substituents in the aryl 2- and 6-positions to approach the metal ions from the axial directions. This leads to drastic low-field shifts of the respective ^{1}H NMR signals, e.g. δ = 7.86 ppm for the isopropyl –CH which comes in close proximity to the low-spin nickel(II) center. The relevance of such low-field NMR resonances of protons close to the axial sites of d^8 metal ions for possible three-center four-electron M···H–C hydrogen bonds involving the filled d_z^2 orbital of the metal ion is discussed. In the present case, attractive M···H interactions are assumed to be of no major significance. This was corroborated by the structure of a further $[L_2Ni_2]^{2+}$ type complex where the anilinomethyl side arms bear only a single 2-isopropyl group, which was found rotated away from the metal. Additional spectroscopic and electrochemical properties of the various complexes are reported.

Introduction

At present, research on di- and oligonuclear transition metal complexes is a flourishing field with major interests focussed on biological mimicry and cooperative phenomena in catalysis and magnetism.[1–4] Among the diverse ligand frameworks that have been designed and employed in order to hold two metal centers in close proximity and to induce the sought-after cooperativity, pyrazole derived species appear particularly suited due to their well-known ability to span adjacent metal ions at a favorable distance of 2.4−4.6 Å.[5,6] Further control of the metal−metal separation, as well as of the steric and electronic properties of the individual metal ions, can be achieved by appropriate chelating side arms attached to the 3- and 5-positions of the heterocycle,[7,8] usually giving rise to either bis(μ-pyrazolato) bridged species L_2M_2 (**A**, Scheme 1)[9–15] or LM_2X complexes featuring secondary bridges within the dimetallic pocket (**B**).[16–24]

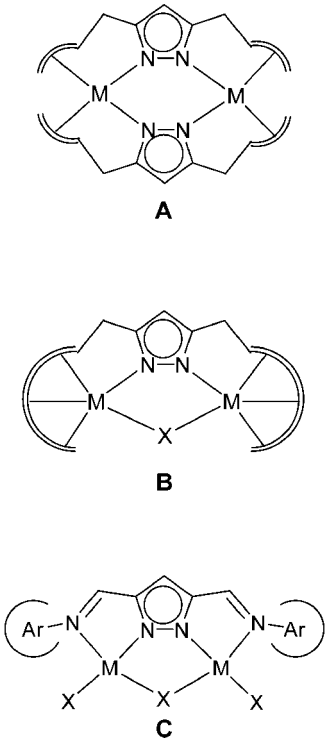

Scheme 1. Different types of dinuclear complexes with multifunctional pyrazolate-based ligands

[a] Institut für Anorganische Chemie der Georg-August-Universität Göttingen
Tammannstraße 4, 37077 Göttingen, Germany
Fax: (internat.) + 49-(0)551-393063
E-mail: franc.meyer@chemie.uni-goettingen.de
[b] Anorganisch-Chemisches Institut der Universität Heidelberg
Im Neuenheimer Feld 270, 69120 Heidelberg, Germany
[‡] New address: Crompton GmbH,
Ernst-Schering-Straße 14, 59192 Bergkamen, Germany

  DOI: 10.1002/ejic.200300778

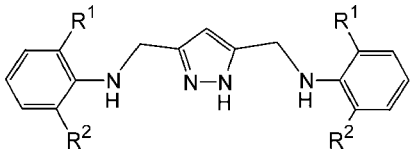

Scheme 2. Ligands used in this study[27]

In this contribution we report on the effects that coordinating versus non-coordinating co-ligands as well as bulky substituents at the chelating side arm donor atoms of L_2M_2 type compounds have on the solid-state structures, and we will particularly focus on unusual metal-ligand interactions that arise from the steric crowding in such systems. Nickel(II) and palladium(II) complexes of ligands $[L^1]^-$, $[L^2]^-$ and $[L^3]^-$ (Scheme 2) were initially prepared with the aim of providing diamine analogues of the bis(α-diimine) type dinuclear compounds **C**.[25,26] However, with $[L^1]^-$, $[L^2]^-$ and $[L^3]^-$, complexes of the type L_2M_2 (**A**) were favored in all cases, irrespective of the M:L ratio employed.

Results and Discussion

Syntheses of all complexes were readily achieved by deprotonation of the respective ligand precursor (HL^1, HL^2, or HL^3)[27] with one equivalent of KO*t*Bu in THF and subsequent addition of the respective metal salt.

Complexes of $[L^1]^-$: Solid-State Structures and Magnetic Properties

From the reaction between HL^1 and $NiCl_2{\cdot}6H_2O$, two structurally isomeric complexes $[L^1_2Ni_2Cl_2]$ (**1**) and $[L^1_2Ni_2]Cl_2$ (**2**) were obtained from acetone and CH_2Cl_2 solutions, respectively. The molecular structures of **1** and **2** are depicted in Figure 1 and 2 together with selected interatomic distances and bond angles.

In the green compound **1**, both nickel ions exist in roughly square-pyramidal coordination environments (τ = 0.11 and 0.18 for Ni1 and Ni2, respectively)[28] with the Cl ligands in axial positions. The metal ions are displaced slightly out of the planes of the basal N-donor atoms towards the axial ligands, which are located on opposite sides of the bimetallic framework defined by the two $\{N_4\}$ chelate ligands. As expected, the distances between the nickel and the coordinating amine N atoms are around 10% longer than the Ni−N(pyrazolate) distances [2.158(3) −2.224(3)Å versus 1.956(3) −1.978(3) Å]. The ligand side arm aryl substituents in **1** are oriented almost perpendicular to the plane of the pyrazolate, and hence perpendicular to the plane of the coordination framework. Due to the space required by the axial co-ligand, the adjacent aryl rings are pushed away from the chloride towards the back side of the dimetallic array. This situation has to balance two competing steric interactions: either some *ortho* methyl groups of the aryl substituents come quite close to the Cl atom [e.g. *d*(C21···Cl2) = 3.718 Å, *d*(C42···Cl1) = 3.942 Å], or the other *ortho* methyl groups are forced to approach the nickel ion from the reverse [C11, C41, C20, C32; *d*(Ni···C_{CH3}) = 3.482−3.783 Å]. In order to avoid an energetically unfavorable full eclipse of the opposing pairs of aryl rings, the respective five-membered chelate rings adopt different conformations (Scheme 3). For each nickel, one chelate ion is almost planar (at N3 and N4), while the second ring adopts an envelope conformation with the aryl groups in either an axial (N8) or an equatorial position (N7).

In the red compound **2**, the chloride ions are detached from their metal atoms, but they still remain associated with the complex via NH···Cl hydrogen bonds [*d*(N3···Cl5) =

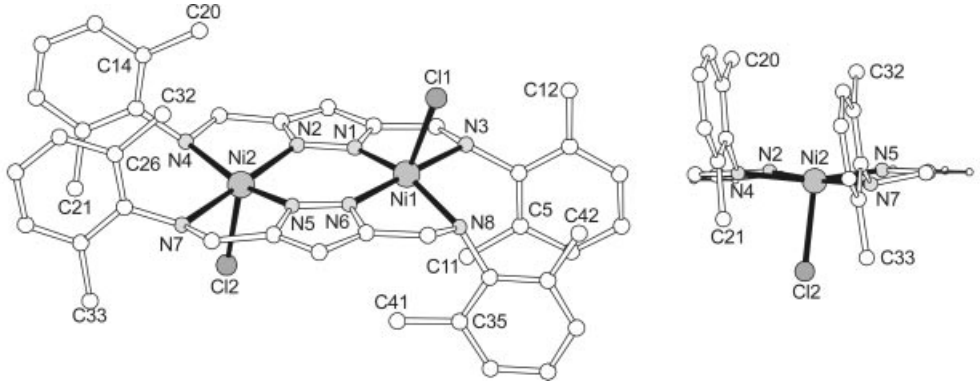

Figure 1. Molecular structure of **1**; in the interests of clarity all hydrogen atoms have been omitted; selected interatomic distances (Å) and bond angles (°): Ni1−N6 1.964(3), Ni1−N1 1.978(3), Ni1−N3 2.183(3), Ni1−N8 2.224(3), Ni1−Cl1 2.339(1), Ni1···Ni2 3.960, Ni2−N2 1.956(3), Ni2−N5 1.977(3), Ni2−N7 2.158(3), Ni2−N4 2.199(3), Ni2−Cl2 2.331(1); C5−C11−Ni1 82.2, C35−C41−Ni1 85.7, C14−C20−Ni2 82.3, C26−C32−Ni2 86.9

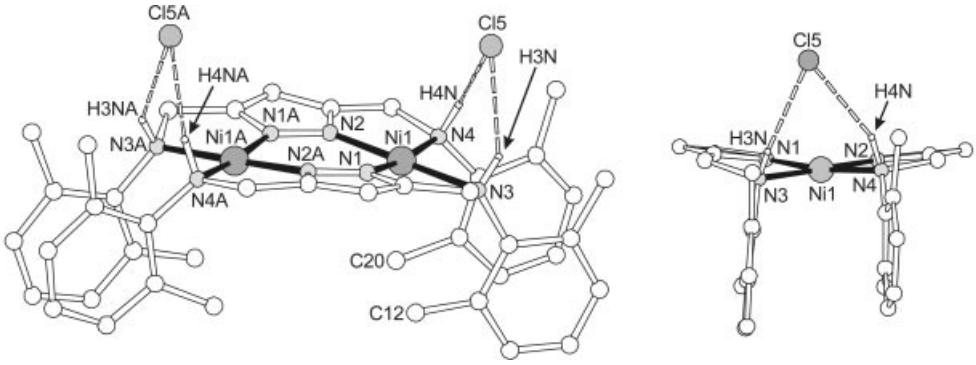

Figure 2. Molecular structure of **2**; in the interests of clarity all but the *N*-bound hydrogen atoms have been omitted; selected interatomic distances (Å) and bond angles (°): Ni1−N2 1.839(2), Ni1−N1 1.843(2), Ni1−N3 1.979(2), N1−N4 1.999(2), Ni1···Ni1A 3.830(8), Ni1···Cl5 3.214(2), N3−Cl5 3.160, N4−Cl5 3.229; N2−Ni1−N3 178.27(8), N1−Ni1−N4 172.48(9)

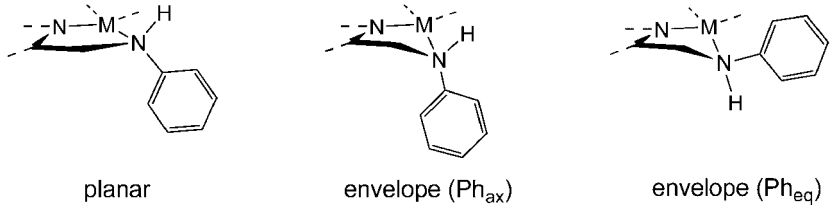

Scheme 3. Conformations of five-membered chelate rings

3.160 Å, *d*(N4···Cl5) = 3.229 Å]. The Ni···Cl distance is 3.214 Å [versus 2.339(1)/2.331(1) Å in **1**], i.e. clearly out of the bonding range, which leaves the metal ions in an approximately square-planar {N_4} environment and slightly decreases the Ni···Ni separation compared with **1** [3.830(1) Å versus 3.960(1) Å]. Due to the H-bonding pattern of the chloride ions, which are both located on one side of the bimetallic array, all aryl rings are directed downwards to the opposite side. Again, this forces two *ortho* methyl groups in close proximity to the metal ions [*d*(Ni···C12) = 3.417 Å, *d*(Ni···C20) = 3.284 Å]. Similar to the situation in **1**, the five-membered chelate rings feature different conformations in order to avoid a fully eclipsed stacking of the aryl groups. All Ni−N bond lengths are significantly shorter than in **1**, in accordance with the lower coordination number and the different spin state, i.e. a high-spin d^8 configuration in **1** compared with a low-spin configuration in **2**. It remains unclear, why the Cl^- ions in **2** are located on the same side of the bimetallic platform, while the Cl ligands in **1** are found on opposite sides.

The aryl rings facing each other in complexes **1** and **2** do not adopt an exact face-to-face alignment, but something of a slipped facial arrangement. To characterize the π-π stacking, one usually considers parameters such as the distance between, and the relative tilting of the planes of opposite aryl rings as well as the centroid−centroid distance (CC), and the angle between the centroid-centroid vector and the ring normal to one of the aryl planes.[29] In **1**, the planes are tilted by 4.3/5.1°, the CC distance is 3.81/4.15 Å, and the offset of the centroids is 1.41−2.13 Å, hence the distance between the centroid and the plane of the opposite aryl ring amounts to 3.49−3.57 Å. These latter values are in the typical range for interplanar distances of π-π stacked aromatic groups (3.3−3.8 Å).[29] In **2**, tilting of the aryl planes relative to each other is similar (6.2°), but the CC distance is somewhat shorter (3.55 Å) and the two rings are less displaced (offset 1.05/1.17 Å). Again, the interplanar separation of the aromatic groups (3.35/3.39 Å) is in the usual range.

The paramagnetic nature of **1** and the diamagnetic nature of **2** were confirmed by magnetic measurements. Temperature dependent data for the molar magnetic susceptibility and the effective magnetic moment of **1** are shown in Figure 3.

From ca. 4.7 B.M. at 300 K, the magnetic moment gradually decreases upon lowering the temperature, while the susceptibility curve exhibits a sharp maximum at around 60 K which is indicative of significant antiferromagnetic coupling between the two nickel(II) centers. Modeling the experimental data by the standard expression for the isotropic spin-Hamiltonian $H = -2J \cdot S_1 \cdot S_2$ (with $S_1 = S_2 = 1$) including a molar fraction p of uncoupled paramagnetic impurity [Equation (1)][4,30,31] yielded $J = -23.2\ cm^{-1}$, $g = 2.39$ and $p = 1.9\%$.

$$\chi = \chi_{dim}(1 - p) + 2\chi_{mono}p + 2N_{\alpha'} \quad (1)$$

The intra−dimer exchange term J proved to be the dominant contribution because a good quality fit was obtained despite the neglect of both a zero-field splitting parameter D as well as an inter−dimer interaction $z'J'$.[32] Relatively few bis(μ-pyrazolato)-bridged high-spin dinickel(II) complexes have been previously structurally charac-

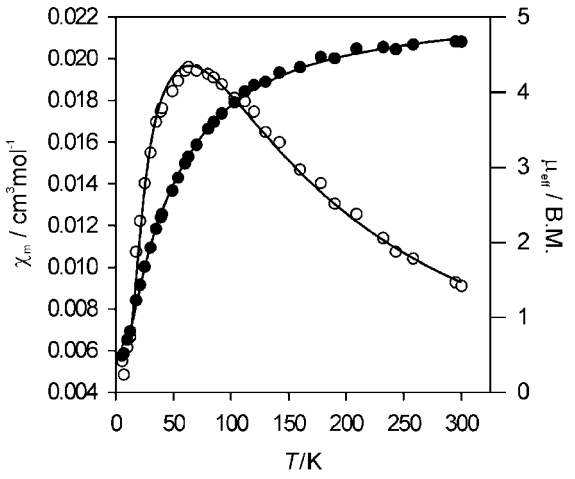

Figure 3. Temperature dependence of the molar magnetic susceptibility (open circles) and magnetic moment (solid circles) for **1**; the solid line represents the calculated fit (see text)

terized,[22,33,34] and even fewer have been studied with respect to their magnetic properties,[35] which precludes any definite magneto-structural correlations at the present stage. However, the rather large magnetic coupling in **1** is certainly due to the high degree of planarity of the $Ni(NN)_2Ni$ scaffold, in accordance with the magneto-structural trends observed in bis(μ-pyrazolato) dicopper(II) chemistry.[36,13]

The controlled synthesis of a complex with low-spin square-planar metal ions was achieved by treatment of $[L^1]^-$ with $[Ni(H_2O)_6](ClO_4)_2$. The molecular structure of the resultant compound **3**, obtained in crystalline form from acetonitrile/diethyl ether, is depicted in Figure 4.

The first coordination sphere of the nickel ions in **3** is quite similar to that in **2**, but less distorted with both metal centers nested within the plane of an overall planar framework. All five-membered chelate rings are roughly planar in this case. In the absence of any steric requirements of chloride counter-anions or co-ligands, the two aryl rings on both ends of **3** do not face each other, but one of them is pointing above and the other below the coordination plane. This gives rise to the sterically more favorable isomer **E** with approximate (non-crystallographic) C_{2h} symmetry (Scheme 4), in contrast to the C_{2v} isomer **D** that is imposed by the four NH···Cl bonds in **2** and the C_{2h} isomer **F** found for **1**. Note that the chiral D_2 isomer **G**, which should be quite similar to the C_{2h} isomer **E** in terms of steric effects, was not observed (neither were any isomers of lower symmetry). The C_{2h} isomer can be described as a *meso* form with an (*R*,*S*)(*S*,*R*) configuration of the four stereogenic N atoms, while the D_2 system represents a pair of enantiomers with (*R*,*R*)(*R*,*R*) or (*S*,*S*)(*S*,*S*) configurations. Interestingly, the *ortho* methyl groups in **3** are even closer to the nickel ions than in **2**, approaching from both axial directions [*d*(Ni···C11) = 3.033 Å, *d*(Ni···C32) = 3.110 Å].

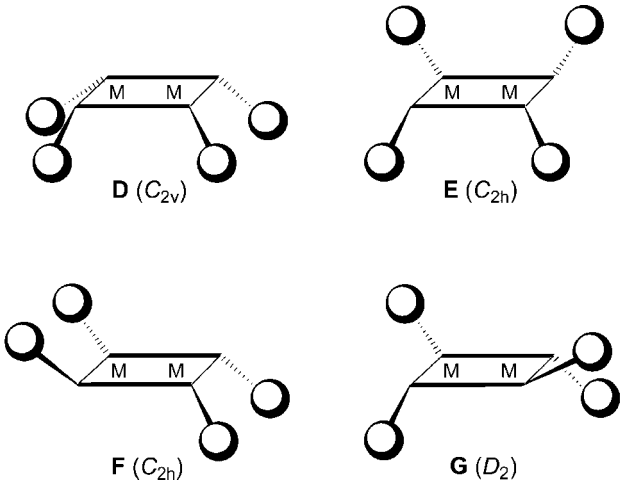

Scheme 4. Different stereoisomers of the $[L_2M_2]^{2+}$ platform (M = Ni, Pd); the balls represent the bulky aryl substituents

The set of dinickel complexes **1**–**3** exemplifies the influence of co-ligands (in this case Cl^-) within the first or second coordination shell on the structural features of the bimetallic scaffold. The sequence given in Figure 5 may

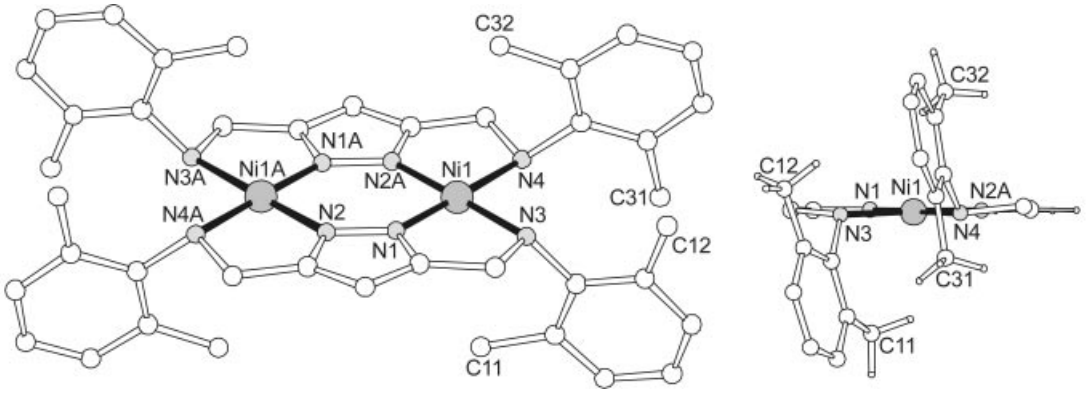

Figure 4. Molecular structure of the cation of **3**; in the interests of clarity only the hydrogen atoms of the methyl groups are shown in the right part; selected interatomic distances (Å) and bond angles (°): Ni1–N2A 1.834(2), Ni1–N1 1.843(2), Ni1–N3 1.957(1), Ni1–N4 1.972(2), Ni1···Ni1A 3.841, C11···Ni1 3.033, C32···Ni1 3.110; N2A–Ni1–N3 179.17(7), N1–Ni1–N4 179.08(7)

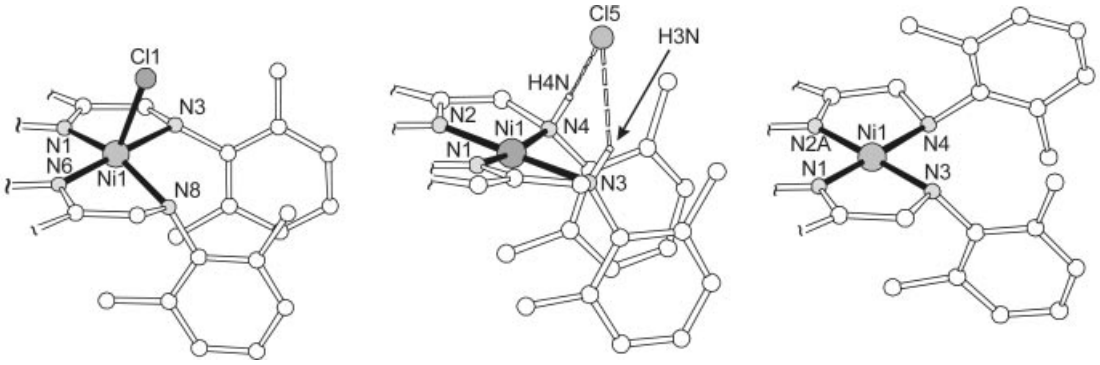

Figure 5. Comparative view of the Ni coordination in **1**, **2** and **3** with the chloride in the inner coordination sphere (**1**), outer coordination sphere (**2**), and without chloride (**3**)

then be viewed as a set of snapshots of the chloride dissociation process. The accompanying spectroscopic characteristics and solution properties of **1**−**3** are discussed below.

For comparison, a dipalladium complex **4** was prepared from $[L^1]^-$and $[Pd(NCMe)_4](BF_4)_2$ and crystallized (in low yield) from dichloromethane/light petroleum. The molecular structure of its cation is basically analogous to that of **3**. However, closer inspection reveals subtle differences which are revealed in Figure 6. In **4**, all chelate rings are more distorted towards an envelope conformation, which brings the adjacent aryl rings to partly stand opposite to each other and to move into the coordination plane. We believe two effects to be responsible for this. Firstly, the larger ionic radius of palladium(II) compared with nickel(II) (0.86 versus 0.72 Å) induces a larger separation between the aryl rings, allowing them to relax towards a more eclipsed stacking. Secondly, the larger palladium ion interferes more strongly with the *ortho* methyl groups, thus enforcing somewhat longer Pd···C distances (3.428 and 3.486 Å) in the axial positions of the metal center and pushing away the substituents. The parallel-displaced arrangement of the aromatic groups in these complexes (as well as in complexes **5**−**7**, see below) means that the interaction is more of the C−H···π type and driven by the known π-σ attraction, while π-π stacking is not favored.[29]

Complexes of $[L^1]^-$ in Solution

A solution of **1** (or, **2**) appears green in CH_2Cl_2 but red in MeCN, and dilution of a THF solution also causes a gradual change from green to red. This change in color is consistent with the crystallographic findings. In non-polar solvents and in concentrated solutions, the position of the equilibrium between **1** and **2** is shifted towards the neutral species $[L^1_2Ni_2Cl_2]$ and the more ionic $[L^1_2Ni_2]Cl_2$ is the less soluble compound that crystallizes from the solution. On the other hand, polar solvents such as MeCN or acetone favor the ionic form $[L^1_2Ni_2]Cl_2$, and the neutral **1** now becomes less soluble and precipitates first.

In order to obtain some further insight into these equilibria, a solution of the Cl-devoid complex **3** in CH_2Cl_2/MeCN (1:1) was titrated with $[(n\text{-hex})_4N]Cl$ and the mixture was analyzed by UV/Vis spectroscopy. Even in the presence of an excess of chloride, **3** was not fully converted into **1** in that solvent mixture. The absence of clear isosbestic points indicates the presence of more complex equilibria presumably involving, inter alia, species such as $[L^1Ni_2Cl]^+$.

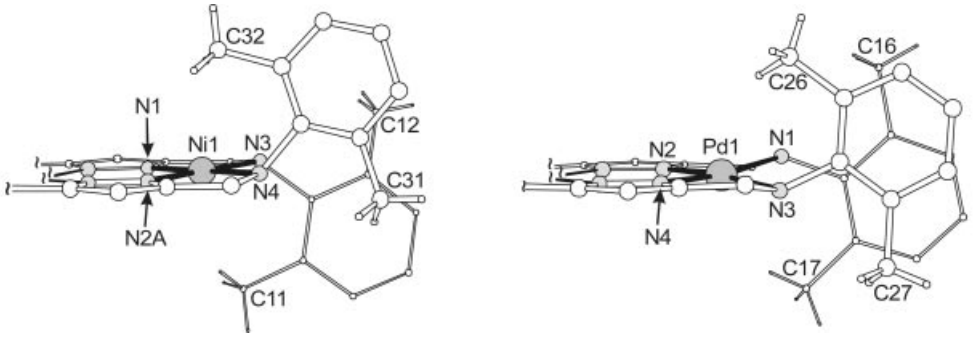

Figure 6. Comparative view of fragments of the molecular structures of **3** and **4**; in the interests of clarity only those hydrogen atoms bound to the methyl groups are shown; selected interatomic distances (Å) and bond angles for **4** are (°): Pd1−N2 1.969(2), Pd1−N4 1.970(2), Pd1−N1 2.110(2), Pd1−N3 2.123(2), Pd1···Pd1A 3.954, Pd1···C17 3.486, Pd1···C26 3.428; N4−Pd1−N1 173.49(8), N2−Pd1−N3 173.95(8)

Solid state UV/Vis/NIR spectra of **1**−**3** were recorded for comparison and are depicted in Figure 7. As expected for five-coordinate high-spin nickel(II) ions, **1** shows a series of absorptions, including the broad band at around 1980 nm, that should correspond to the $^3B_1 \rightarrow {}^3E$ transition in idealized C_{4v} symmetry. The two distinct bands at 328 and 502 nm for **3** can be assigned to the $^1A_{1g} \rightarrow {}^1B_{1g}$ and $^1A_{1g} \rightarrow {}^1A_{2g}$ transitions of low-spin nickel(II) in an idealized D_{4h} environment, where the latter gives a reasonable value of the ligand field splitting, $\Delta \approx 20000\ cm^{-1}$.[37] The similarity of the band positions for **1** and **3** in the range 300−1000 nm with those observed in solution confirms that the overall structures elucidated by X-ray crystallography are essentially retained in solution.

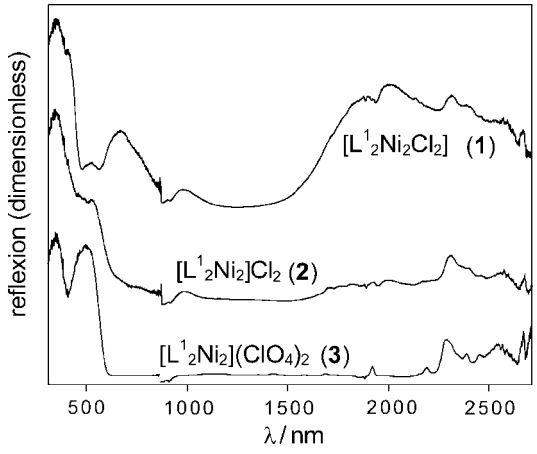

Figure 7. Solid state UV/Vis spectra of the dinickel complexes **1**, **2** and **3**

^1H NMR spectroscopy of diamagnetic **3** revealed unusual chemical shifts for the *ortho* methyl groups of the aryl rings (Figure 8; all signals have been unambiguously assigned by a series of 2D NMR experiments). While the CH_3 resonance appears at δ = 2.29 ppm in HL[1], the spectrum of **3** shows one signal shifted to higher field at δ = 1.08 ppm and two signals (of different intensities) at very low field, i.e. at δ = 4.17 and 4.20 ppm. These features can be rationalized by considering the positions of the methyl groups and, as is clearly seen in Figure 4, the high-field shifts of H12A−C and H31A−C are due to their location within the field of the ring current of the opposing aryl rings, while the deshielding of H11A−C and H32A−C results from their proximity to the filled d_z^2 orbital of the nickel(II) ion. The occurrence of two closely spaced resonances for the latter protons has been tentatively attributed to the presence of different isomers in solution, such as the C_{2h} and D_2 forms sketched in Scheme 4. These effects are even more pronounced in the case of complexes of $[L^2]^-$ and are discussed in more detail below. The diastereotopic nature of the CH_2 protons of the five-membered chelate rings is reflected by two well-separated sets of signals centered at δ = 3.43 and 4.15 ppm.

^1H NMR spectra of the palladium complex **4** in CD_2Cl_2 only show very broad resonances over a wide temperature range, presumably indicating a variety of dynamic and dissociative processes.

Complexes of $[L^2]^-$: Solid-State Structures and Spectroscopy

Similar to the preparation of **3** and **4**, the dinickel and dipalladium complexes $[L^2_2Ni_2](ClO_4)_2$ (**5**) and $[L^2_2Pd_2](BF_4)_2$ (**6**) were obtained by treatment of $[L^2]^-$ with $[Ni(H_2O)_6](ClO_4)_2$ or $[Pd(NCMe)_4](BF_4)_2$, respectively. Single crystals were grown from acetone/ethanol/light petroleum (**4**) or dichloromethane/light petroleum (**5**) and analyzed by X-ray crystallography. Both **5** and **6** crystallize in the triclinic space group $P\bar{1}$, and molecular structures of their cations are shown in Figure 9.

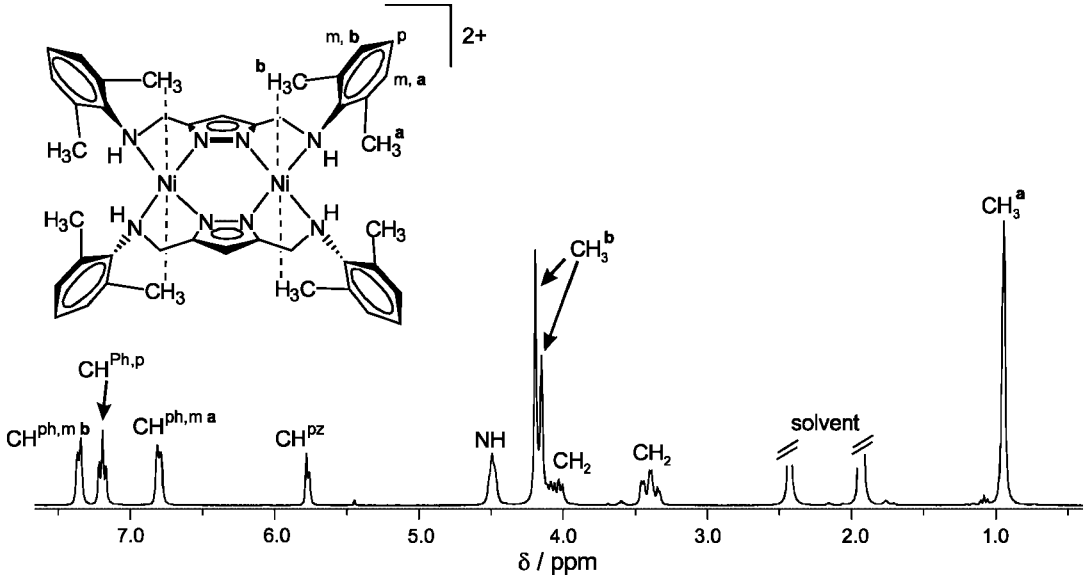

Figure 8. ^1H NMR spectrum of complex **3** in CD_3CN at 300 MHz and 293 K; the dashed lines in the graphical representation of **3** are not meant to indicate bonds

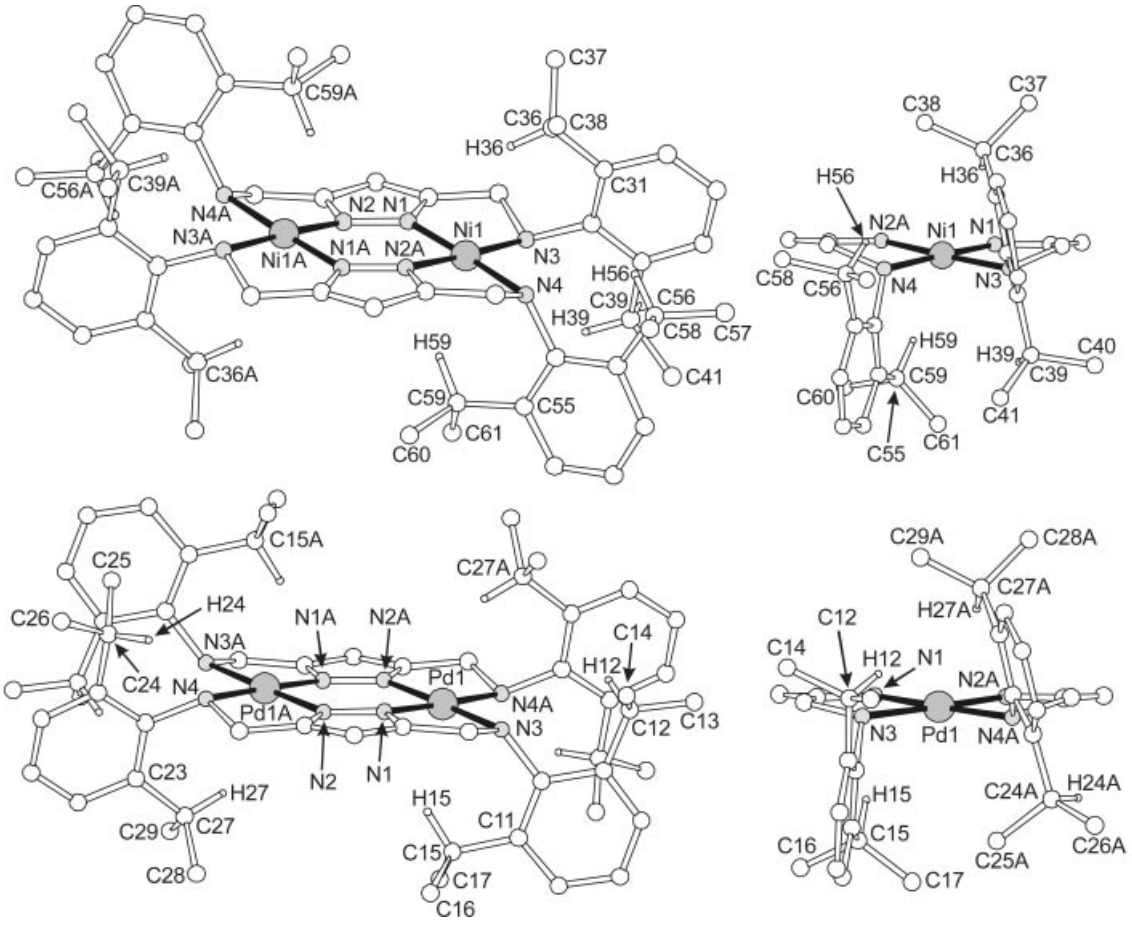

Figure 9. Molecular structures of the cations of **5** (top) and **6** (bottom); in the interests of clarity only a few hydrogen atoms are shown; selected interatomic distances (Å) and bond angles (°) for **5**: Ni1−N1 1.835(3), Ni1−N2A 1.848 (3), Ni1−N3 1.967(3), Ni1−N4 1.974(3), Ni1···Ni1A 3.842, C36···Ni1 3.269 C59···Ni1 3.114; N2A−Ni1−N3 177.25(11), N1−Ni1−N4 178.00(12); selected interatomic distances (Å) and bond angles (°) for **6**: Pd1−N1 1.968(3), Pd1−N2A 1.971(3), Pd1−N3 2.114(3), Pd1−N4A 2.123(3), Pd1···Pd1A 3.997, C15···Pd1 3.454, C27A···Pd1 3.377; N2A−Pd1−N3 176.09(12), N1−Pd1−N4A 176.19(12)

All metal ions are found in roughly SP-4 coordination environments. Due to the steric pressure exerted by the bulky 2,6-diisopropylphenyl substituents, however, the coordination planes of the metal ions are tilted by ca. 10° (**5**) or 8° (**6**) with respect to the planes of the pyrazolate heterocycles. The chelate rings adopt an envelope conformation with one aryl substituent in an axial position and one in an equatorial position for each half of the molecule (cf. Scheme 3). These structural features cause the methine proton of one isopropyl group of every aryl substituent to approach considerably close to the proximate metal ion from the axial direction [*d*(C36···Ni) = 3.269 Å and *d*(C59···Ni) = 3.114 Å in **5**, *d*(C15···Pd) = 3.454 Å and *d*(C27···Pd) = 3.377 Å in **6**]. The consequences for the ^{1}H NMR chemical shifts of these particular protons should be more pronounced than in **3**, since rotation is hindered for the isopropyl groups in **5**, while rotation of the methyl groups causes an averaging of the effect in **3**. The expected four CH_3 resonances for the non-equivalent isopropyl groups in **5** were seen in the low temperature (193 K) ^{1}H NMR spectrum in CD_2Cl_2 (Figure 10). Signals have been assigned based on a series of 2D NMR experiments ({^{1}H^{13}C}HSQC and {^{1}H^{13}C}HMBC), and the methine resonances of the isopropyl groups were found either at extremely low field (δ = 7.86 ppm; CH^B close to the nickel ion) or at very high field (δ = 1.86 ppm; CH^A opposing the proximate aryl ring) compared with the free ligand HL^2 (δ = 3.33 ppm at room temp.). At 193 K, the CH_2 protons at δ = 3.40 and 4.13 ppm showed a geminal coupling of ^2J = 10 Hz, in accordance with a fixed conformation of the five-membered chelate rings. At higher temperatures, a second set of resonances gradually developed, which were most clearly observed for the isopropyl-CH_3 groups and were also evident from the splitting of the signal at around 5.9 ppm for the pyrazolate H^4 proton (CH^{pz}). At 293 K, a 1:1 ratio of the two isomers was obtained. These different isomers have been tentatively assigned to the C_{2h} and D_2 forms of the bimetallic framework, where the two aryl substituents of each ligand are either on the same (C_{2h}) or on opposing sides (D_2). Interconversion was apparently rapid and may proceed either via a short-lived dissociation of the Ni−N bonds and inversion of the intermediate free amine, or via a sequence of deprotonation and inverse protonation of the *N*-bound protons.

In CD_3CN at higher temperatures all ^{1}H NMR signals of **5** became broad, except for the *para* protons of the aryl

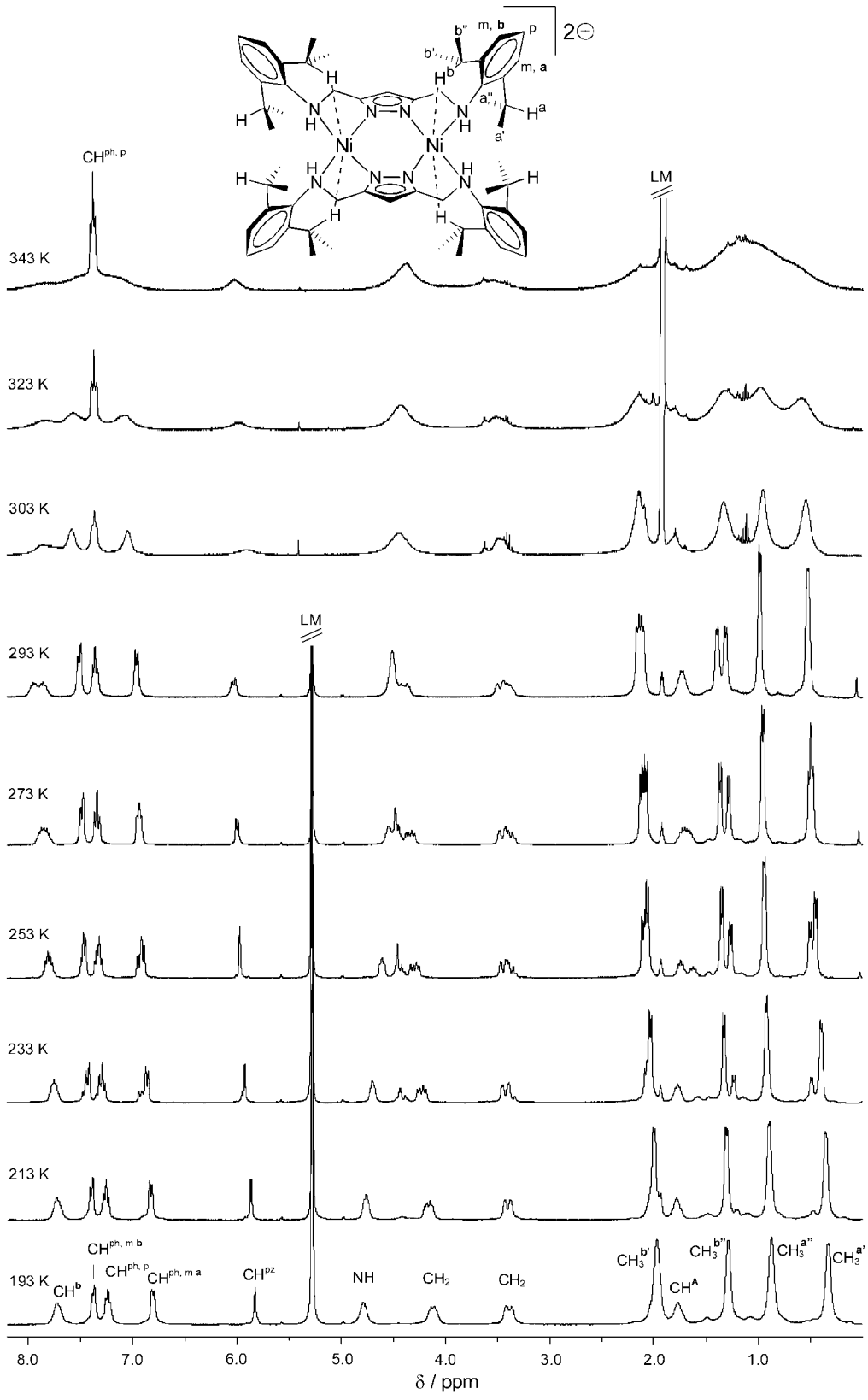

Figure 10. Temperature dependent ^{1}H NMR spectra of complex **5** in CD_3CN (303−343 K) and CD_2Cl_2 (193−293 K) at 300 MHz; the dashed lines in the graphical representation of **5** do not indicate bonds

groups. We assume dissociative processes according to Scheme 5 to be responsible for this phenomenon, which may also support the former explanation for the stereoisomer interconversion discussed above. Similar characteristics were observed for the ^{1}H NMR spectrum of **6**, but with a somewhat less pronounced deshielding of its CH^B protons.

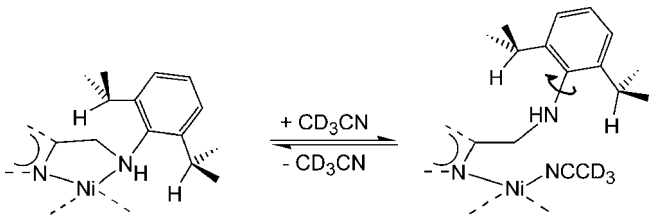

Scheme 5. Possible solvent-assisted side arm dissociation

When **5** was treated with two equivalents of HL^1, formation of **3** and the heteroleptic complex $[L^1L^2Ni_2]$ $(ClO_4)_2$ (**7**) was observed within minutes. However, ligand exchange did not proceed to completeness, and equilibrium was reached at ca. 70% exchange. The mixed-ligand species **7** could be prepared directly by treatment of a 1:1 mixture of $[L^1]^-$ and $[L^2]^-$ with two equivalents of $[Ni(H_2O)_6](ClO_4)_2$. Single crystals were obtained from a MeCN/diethyl ether solution and were analyzed by X-ray crystallography. The molecular structure of the cation of **7** is depicted in Figure 11 together with selected atom distances and bond angles.

In **7**, the two nickel ions were found in subtly different environments. While the coordination sphere of Ni2 is almost square-planar, Ni1 shows a slight tetrahedral distortion. Five-membered chelate rings of all possible conformations (planar, λ-twist, δ-twist) are present in **7**. The two pyrazolate heterocycles are tilted by 12.1° with respect to each other.

While the steric strain in **7** is somewhat relieved compared with **5**, the distances of the isopropyl CH atoms to the nickel ions are rather similar [*d*(Ni2···C48) = 3.230 Å and *d*(Ni···C32) = 3.200 Å versus 3.114 and 3.269 Å in **5**]. Also, the distances between the nickel atoms and the methyl groups of $[L^1]^-$ are similar to those in the homoleptic compound **3** (3.082 and 3.119 Å in **7** versus 3.033 and 3.110 Å in **3**).

The ^{1}H NMR spectrum of **7** is reminiscent of an overlay of the individual spectra of **3** and **5**. Chemical shifts of all signals assigned to the $[L^1]^-$ and $[L^2]^-$ ligand protons are quite similar to those in the homoleptic analogues. Deshielding of the isopropyl CH protons is only slightly less pronounced than in **5** (7.20 and 7.40 ppm versus 7.86 ppm; again, the two separate resonances are presumably due to the presence of different isomers in solution).

A ^{1}H NMR spectrum of the bulk crystalline material obtained from acetonitrile/diethyl ether by the synthetic procedure described above shows a $[L^1]^-$:$[L^2]^-$ ratio of approximately 2:1. We assume that **3**, **5** and **7** are initially formed in a statistical 1:1:2 mixture. Upon crystallization, however, both the less soluble **3** and **7** precipitate, while **5** remains in solution. As a consequence, the isolated crystalline material represents a 1:2 mixture of **3** and **7**, which gives rise to the observed 2:1 ratio of $[L^1]^-$:$[L^2]^-$ in the NMR spectroscopic analysis.

Comparative Discussion of Unusual ^{1}H NMR Shifts and Synthesis of a Complex of $[L^3]^-$

Close contacts between d^8 metal ions Pd^{II} and Pt^{II} in square-planar complexes and N−H or O−H bonds located above or below the coordination plane have been observed in several cases and investigated in detail.[38–41] Similar contacts with C−H bonds are less recognized and usually involve sp or sp^2 carbon atoms.[38,42–50] For some systems, these contacts have been interpreted in terms of three-center four-electron M···H−N and M···H−C hydrogen bonds involving the filled d_{z^2} orbital of the metal ion (Scheme 6), in contrast to three-center two-electron agostic interactions.

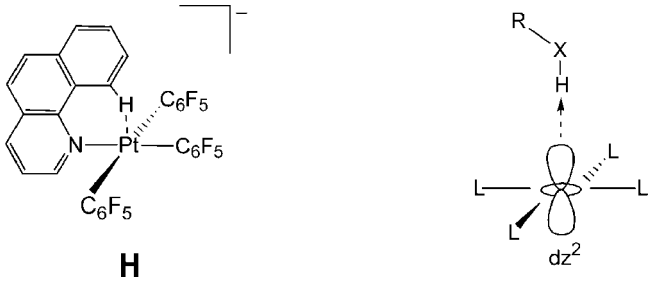

Scheme 6. Three-center four-electron M···H−X hydrogen bonds[50]

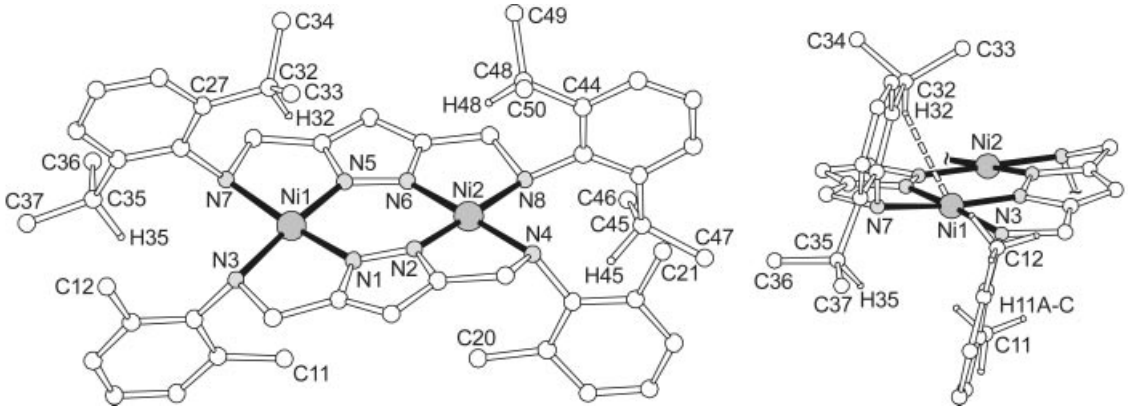

Figure 11. Molecular structure of the cation of **7**; in the interests of clarity only a few hydrogen atoms are shown; selected interatomic distances (Å) and range of selected bond angles (°): Ni1−N1 1.846(4), Ni1−N5 1.852(4), Ni1−N7 1.973(4), Ni1−N3 1.980(4), Ni2−N6 1.844(4), Ni2−N2 1.849(4), Ni2−N4 1.956(4), Ni2−N8 1.984(4), Ni1···Ni2 3.848, C32···Ni1 3.200, C11···Ni1 3.082, C20···Ni2 3.119; C48···Ni2 3.230; N1−Ni1−N7 173.5(2), N5−Ni1−N3 174.7(2), N6−Ni2−N4 178.6(2), N2−Ni2−N8 178.4(2)

While a significant downfield ^{1}H NMR shift for an H atom in the vicinity of the metal is characteristic for such contacts (agostic interactions are typified by a large upfield shift), it does not provide conclusive evidence for the presence of an attractive M···H interaction. ^{195}Pt−^{1}H coupling constants are a much better indicator, and large values for $^1J_{Pt,H}$ have been observed, e.g. $^1J_{Pt,H}$ = 69 Hz in **H**.[49] Unfortunately no stable, well-defined platinum(II) complexes $[L_2Pt_2]^{2+}$ could be isolated with $[L^1]^-$ and $[L^2]^-$.

Even in the possible presence of weak attractive M···H components, however, these hydrogen bonds have to be in balance with significant repulsive forces, and X-ray crystal structures for many of the systems reported in the literature reveal strained ligand geometries, often in order to relieve the interactions. A detailed molecular mechanics study has supported the view that the axial M···H interactions are mainly repulsive in nature.[51] While we cannot rule out a minor attractive contribution to the M···H−C interaction for the present pyrazolate-based dinuclear nickel(II) and palladium(II) complexes, we believe that the Ni···H and Pd···H interactions are basically repulsive and that the H atoms are forced to lie close to the metal ions simply because of geometric constraints due to the bulky ligand substituents. This has been further corroborated by the structure of the dinickel complex of $[L^3]^-$ described below. It should also be noted that the M−H−C angles in **1**−**7** (ca.140°) are more acute by 20°−30° than in those complexes with a confirmed M···H bonding interaction.[42]

Ligand $[L^3]^-$ which bears only a single *ortho* isopropyl substituent on all of its aryl groups was expected to provide clear evidence for the absence or presence of an attractive M···H−C interaction, since the isopropyl substituent might be oriented away from the metal ion or towards the axial coordination sites. The former proved to be the case, as revealed by the X-ray analysis of single crystals of $[L^3_2Ni_2](ClO_4)_2$ (**8**), which could be obtained from propionitrile/diethyl ether. In **8**, both nickel ions were again found in square planar $\{N_4\}$ coordination environments with almost planar five-membered chelate rings, and all bond lengths are in the expected regions (Figure 12). For each ligand $[L^3]^-$, the aryl substituents are on the same side of the coordination framework (isomer **E**, Scheme 4), and the isopropyl groups adopt the largest possible distance from the nickel ions. Due to the steric bulk of the isopropyl groups, opposing aryl rings are not fully parallel but are tilted by ca. 30 °C with respect to each other. Overall, the structure of **8** confirms that the system tends to relieve steric strain and to avoid any close M···H−C contacts if possible.

The ^{1}H NMR spectra of **8** in CD_3CN at 293−343 K revealed only very broad signals, indicative of a variety of dynamic processes in solution. The CH protons of the isopropyl groups resonate at ca. 2.3 ppm (at 293 K). Unfortunately, the poor solubility of **8** limits the range of solvents and temperatures for NMR spectroscopy, and satisfactory ^{13}C NMR spectra could not be obtained for **8**.

Electrochemistry

While no anodic processes were observed up to +1.8 V (all potentials relative to the SCE), the low-spin dinickel(II) complexes **3**, **5**, and **8** as well as the dipalladium complex **6** can be electrochemically reduced in acetonitrile or dichloromethane, respectively. Figure 13 depicts their cyclic voltammograms.

The dinickel complex **3** shows a reversible reduction at $E_{1/2}$ = −0.94 V, presumably giving the respective mixed-valent $Ni^{I}Ni^{II}$ compound. Further reduction is quasi-reversible with E_p^{red} = −1.25 V. The rather large separation of the two processes of around 130 mV (from an estimated "$E_{1/2}$" = −1.18 V for the second reduction wave) indicates significant stabilization of the mixed-valent species towards disproportionation ($K_{comp.}$ = 1.2 × 10^4).

Reduction of complexes **5** and **8** bearing isopropyl substituents at the aryl groups is quasi-reversible (E_p^{red} = −0.81 and −0.98 V, respectively), followed by a second irreversible process. The fully reduced species gives an oxidative wave at around −0.14 V or −0.30 V in the reverse scan. Apparently, the more sterically demanding isopropyl substituents lead to enhanced lability of the reduced compounds, and the methyl-substituted scaffold in **3** is best suited for accepting an additional electron in the antibonding nickel d_{xy} orbitals within the coordination plane.

The electrochemistry of the dipalladium complex **6** is quite similar to that of **5** (except for the lack of the oxidative wave in the back scan). Unexpectedly, however, the dipalladium complex **4** does not show any cathodic process

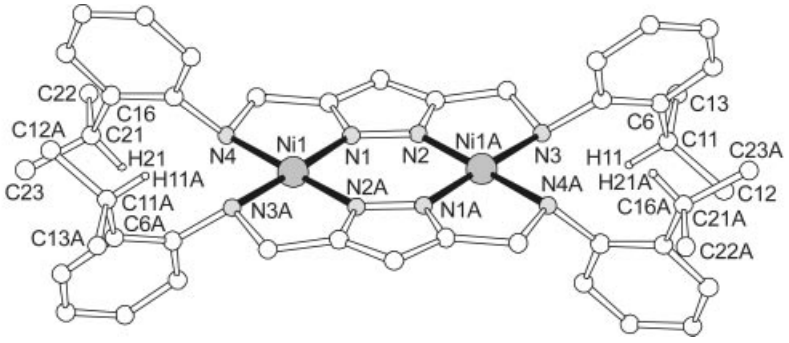

Figure 12. Molecular structure of the cation of **8**; in the interests of clarity only a few hydrogen atoms are shown; selected interatomic distances (Å) and bond angles (°): Ni1−N1 1.8364(12), Ni1−N2A 1.8372(12), Ni1−N3A 1.9697(12), Ni1−N4 1.9719(12), Ni1···Ni1A 3.853(2); N1−Ni1−N3A 178.69(5), N2A−Ni1−N4 176.84(5)

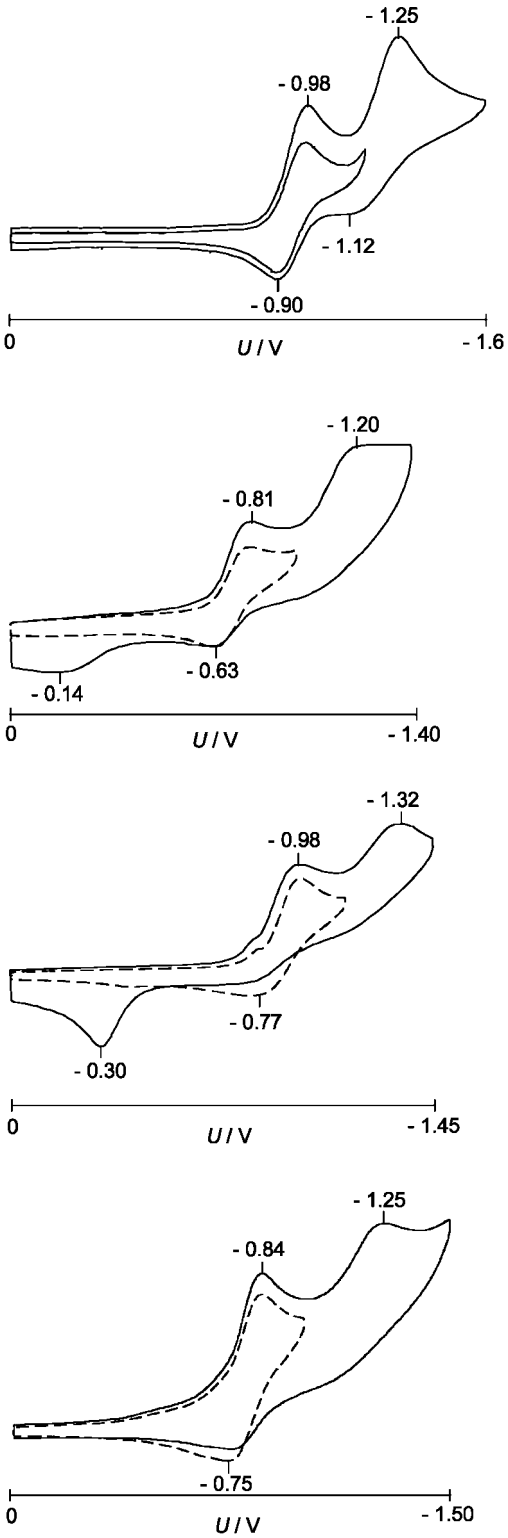

Figure 13. Cyclic voltammograms of **3** (top), **5** (second from top), **8** (second from bottom) and **6** (bottom) recorded on a platinum electrode in MeCN (**3**, **5**, **8**) or CH_2Cl_2 (**6**) containing 0.1 M $NnBu_4^+PF_6^-$; scan speed 200 mVs^{-1}

down to −2.5 V, but an irreversible oxidation at E_p^{ox} = +1.05 V. This corroborates the conclusions drawn from the NMR spectroscopic findings, i.e. the constitution of **4** in solution is most probably not identical to the structure observed in the solid state.

Conclusion

The anilinomethyl-appended pyrazolate ligands $[L^1]^-$, $[L^2]^-$ and $[L^3]^-$ yielded dinuclear type **A** complexes $[L_2M_2]^{2+}$ upon treatment with nickel(II) and palladium(II). Coordinating counter-anions such as chloride can bind to axial sites of the dinickel species in a solvent-dependent process, giving rise to five-coordinate metal ions. In the case of weakly coordinating anions, the metal ions were found in roughly square-planar environments with the structures being dictated by steric requirements due to the bulky aryl substituents. It is noteworthy that all complexes with four-coordinate (square planar) metal ions characterized crystallographically (i.e. complexes **3**, **4**, **5**, **6**, **7** and **8**) feature a (non-crystallographic) C_{2h}-type *meso* arrangement of the aryl groups, while the chiral D_2-type (compare Scheme 4) was not observed in the solid state. Only in the case of **2** was a less sterically favorable C_{2v} isomer enforced by the NH···Cl hydrogen bonds.

The tendency of the aryl groups to avoid each other and not to face each other in close proximity forces the methyl or isopropyl substituents in the aryl 2- and 6-positions to approach the metal ions from the axial directions. This leads to a drastic low-field shift of the respective ^{1}H NMR signals, e.g. δ = 7.86 ppm for the isopropyl-CH that come close to the low-spin nickel(II) ion in $[L^2_2Ni_2]^{2+}$ (**5**). In contrast, the remaining isopropyl-CH comes to lie within the field of the ring-current of the opposing aryl groups and resonates at very high field (δ = 1.86 ppm for **5**).

While the low-field NMR signature of protons close to the axial sites of d^8 metal ions has previously been considered indicative of three-center four-electron M···H−C hydrogen bonds involving the filled d_z^2 orbital of the metal ion, attractive M···H interactions were assumed not to be of major relevance in the present case. This was corroborated by the structure of $[L^3_2Ni_2]^{2+}$, where the single 2-isopropyl groups at each phenyl ring are rotated away from the metal. These phenomena and findings related to the sterically enforced proximity of aliphatic CH bonds to square-planar d^8 metal centers, as reported in the present work, may also be relevant to the characteristics of recent-generation late transition metal catalysts incorporating diamine and diimine ligands, which in many cases also bear bulky aryl substituents.

Experimental Section

General Remarks: Most manipulations were carried out under an dry nitrogen by employing standard Schlenk techniques. Solvents were dried according to established procedures. The ligands were synthesized according to the reported methods,[27] and all other chemicals were used as purchased. Microanalyses: Mikroanalytische Laboratorien des Organisch-Chemischen Instituts der Universität Heidelberg. IR spectra: Perkin−Elmer 983G; recorded as KBr

pellets. UV/Vis spectra: Perkin−Elmer Lambda 19. FAB-MS spectra: Finnigan MAT 8230. NMR spectra: Bruker AC 200 at 200.13 (^{1}H) and 50.32 (^{13}C) MHz, or Bruker DRX 300 at 300.13 MHz (^{1}H) and 75.47 (^{13}C) MHz; solvent signal as chemical shift reference (CD_3CN δ_H = 1.94, δ_C = 118.1/1.2 ppm); where necessary, assignments were based on a series of 2D experiments. Cyclic voltammetry: PAR equipment, (potentiostat/galvanostat 273), in 0.1 M NBu_4PF_6/CH_3CN. Potentials in V on a glassy carbon electrode, referenced to the SCE at ambient temperature. Magnetic measurements: Bruker magnet B-E 15 C8, field controller B-H 15, variable temperature unit ER 4111 VT, Sartorius microbalance M 25 D-S. Experimental susceptibility data were corrected for the underlying diamagnetism.

Caution! *Although no problems were encountered in this work, perchlorate salts are potentially explosive and should be handled with proper precautions.*

General Synthesis of Complexes: For the syntheses of the complexes, the respective ligand (HL^1, HL^2, HL^3; approximately 1 mmol) was dissolved in THF (50 mL) and deprotonated with one equivalent of KO*t*Bu. After the reaction mixture had been stirred for 30 min, one equivalent of the metal salt {$NiCl_2{\cdot}6H_2O$ or $[Ni(H_2O)_6](ClO_4)_2$ or $[Pd(CH_3CN)_4](BF_4)_2$} was added and stirring continued for 15 h. The solvent was then removed under reduced pressure and the residue washed with light petroleum. Pure compounds were obtained by crystallization, i.e. by slow diffusion of light petroleum or diethyl ether into a solution of the complex as detailed below.

Complex 1: Single crystals were obtained from acetone/light petroleum (yield of crystalline material 183 mg; 42%). IR (KBr): $\tilde{\nu}_{max.}$ = 3242 w, 2955 w, 1590 w, 1512 w, 1464 vs, 1436 s, 1379 m, 1302 s, 1251 w, 1191 s, 1093 s, 1042 w, 974 w, 924 m, 900 m, 761 s, 618 w cm^{-1}. M.p. > 240 °C. UV/Vis (CH_3CN): λ (ε) = 226 (16600), 290 sh (7040), 397 (610), 495 (155), 643 nm (35). MS (FAB): *m*/*z* (%) = 819 (30) $[L^1_2Ni_2Cl]^+$, 782 (100) $[L^1_2Ni_2]^+$. $C_{42}H_{50}Cl_2N_8Ni_2$ (855.20): calcd. C 58.99, H 5.89, N 13.10; found C 58.99, H 6.34, N 12.89.

Complex 2: Single crystals were obtained from dichloromethane/light petroleum (yield of crystalline material 114 mg; 26%). IR (KBr): $\tilde{\nu}_{max.}$ = 2944 w, 1590 w, 1522 w, 1465 vs, 1439 s, 1380 m, 1307 s, 1172 s, 1095 s, 947 m, 902 w, 763 s, 724 w, 571 w cm^{-1}. M.p. > 240 °C. UV/Vis (CH_3CN): identical to the spectrum of **1**.

Complex 3: Single crystals were obtained from acetonitrile/diethyl ether (yield of crystalline material 430 mg; 88%). ^{1}H NMR (300 MHz, CD_3CN): δ = 1.08 (s, 12 H, CH_3), 3.37−3.49 (m, 4 H, CH_2), 4.08−4.30 (m, 4 H, CH_2), 4.17, 4.20 (s, 12 H, CH_3), 4.50 (s, 4 H, NH), 5.80 (s, 1 H, CH^{pz4}), 5.81 (s, 1 H, CH^{pz4}), 6.83 (m, 4 H, $CH^{Ph,m}$), 7.21 (t, ^3J = 7.5 Hz, 4 H, $CH^{Ph,p}$), 7.37 (d, ^3J = 7.5 Hz, 4 H, $CH^{Ph,m}$) ppm. ^{13}C NMR (300 MHz, CD_3CN): δ = 16.6 (CH_3), 21.9 (CH_3), 54.5 (CH_2), 97.0 (CH^{pz4}), 129.2 ($CH^{Ph,p}$), 130.1($CH^{Ph,m}$), 132.5 ($CH^{Ph,m}$), 132.9 ($CH^{Ph,m}$), 142.1, 142.4 (C^{ar}), 157.5, 157.6 ($C^{pz3/5}$) ppm. IR (KBr): $\tilde{\nu}_{max.}$ = 3349 m, 3226 m, 2951 m, 1622 m, 1463 m, 1443 m, 1382 w, 1366 w, 1308 m, 1259 w, 1214 w, 1137 vs, 1112 vs, 1084 vs, 951 w, 772 m, 624 s, 418 m cm^{-1}. M.p. > 240 °C. UV/Vis (CH_3CN): λ (ε) = 240 (14820), 300 (10560), 454 (185), 500 nm(175). MS (FAB): *m*/*z* (%) = 883 (90) $[L^1_2Ni_2ClO_4]^+$, 782 (100) $[L^1_2Ni_2]^+$. $C_{42}H_{50}Cl_2N_8Ni_2O_8$ (983.13): calcd. C 51.31, H 5.12, N 11.39; found C 50.83, H 5.41, N 11.44.

Complex 4: A few single crystals were obtained from dichloromethane/light petroleum. MS (FAB): *m*/*z* (%) = 877 (100) $[L^1_2Pd_2]^+$.

Complex 5: Single crystals were obtained from acetone/diethyl ether (yield of crystalline material 170 mg; 28%). ^{1}H NMR (300 MHz, CD_3CN, 233 K), only data for the major isomer are given: δ = 0.39 (d, ^3J = 6.0 Hz, 12 H, CH_3), 0.90 (d, ^3J = 6.0 Hz, 12 H, CH_3), 1.31 (d, ^3J = 6.0 Hz, 12 H, CH_3), 1.86 (sept, ^3J = 6.0 Hz, 4 H, CH*iPr*), 2.05 (d, ^3J = 6.0 Hz, 12 H, CH_3), 3.45 (dd, ^3J = 16.7/4.5 Hz, 4 H, CH_2), 4.31 (dd, ^3J = 16.7/7.8 Hz, 4 H, CH_2), 4.79 (br., s, NH), 5.75 (s, 2 H, CH^{pz4}), 6.98 (d, ^3J = 7.6 Hz, 4 H, $CH^{Ph,m}$), 7.35 (t, ^3J = 7.6 Hz, 4 H, $CH^{Ph,p}$), 7.55 (d, ^3J = 7.6 Hz, 4 H, $CH^{Ph,m}$), 7.86 (sept, ^3J = 6.0 Hz, 4 H, CH*iPr*) ppm. ^{13}C NMR (300 MHz, CD_3CN, 233 K): δ = 22.7 (CH_3), 25.4 (CH_3), 25.8 (CH_3), 26.0 (CH_3), 28.6 (CH*iPr*), 30.9 (CH*iPr*), 57.8 (CH_2), 99.0 ($CH^{pz,4}$), 126.0 ($CH^{Ph,m}$), 127.4 ($CH^{Ph,m}$), 130.2 ($CH^{Ph,p}$), 138.5 ($C^{Ph,1}$), 141.8 ($C^{Ph,2/6}$), 155.8 ($C^{pz3/5}$) ppm. IR (KBr): $\tilde{\nu}_{max.}$ = 3255 m, 2957 s, 2920 m, 2860 w, 1698 m, 1622 w, 1459 s, 1439 s, 1382 m, 1361 m, 1304 s, 1093 vs, 944 w, 931 w, 804 s, 760 m, 623 s, 527 w, 457 w, 419 w cm^{-1}. M.p. > 240 °C. UV/Vis (CH_3CN): λ (ε) = 235 (16560), 298 (8210), 447 (180), 507 nm (195). MS (FAB): *m*/*z* (%) = 1107 (70) $[L^2_2Ni_2(ClO_4)]^+$, 1006 (100) $[L^2_2Ni_2]^+$. $C_{58}H_{82}Cl_2N_8Ni_2O_8$ (1207.62): calcd. C 57.68, H 6.84, N 9.27; found C 57.76, H 7.63, N 9.59.

Complex 6: Single crystals were obtained from dichloromethane/light petroleum (yield of crystalline material 178 mg; 76% after starting from 0.37 mmol HL^2). ^{1}H NMR (300 MHz, CD_2Cl_2): δ = 0.58 (d, ^3J = 6.6 Hz, 6 H, CH_3), 1.04, 1.05 (d, ^3J = 6.6 Hz, 6 H, CH_3), 1.25, 1.30 (d, ^3J = 6.6 Hz, 6 H, CH_3), 1.82 (d, ^3J = 6.6 Hz, 6 H, CH_3), 2.04 (sept, ^3J = 6.6 Hz, 4 H, CH*iPr*), 3.84, 3.95 (dd, ^3J = 16.6/5.3 Hz, 4 H, CH_2), 4.63, 4.71 (dd, ^3J = 16.5/7.8 Hz, 4 H, CH_2), 4.84, 5.00 (sept, ^3J = 6.6 Hz, 4 H, CH*iPr*), 5.90, 6.05 (br., NH), 6.11, 6.22 (s, 2 H, $CH^{pz,4}$), 6.93 (m, 4 H, $CH^{Ph,m}$), 7.30 (m, 4 H, $CH^{Ph,p}$), 7.41 (m, 4 H, $CH^{Ph,m}$) ppm. ^{13}C NMR (300 MHz, CD_2Cl_2): δ = 23.0, 25.3, 25.5, 25.6, 25.8 (CH_3), 28.4 (CH*iPr*), 28.8 (CH*iPr*), 59.8 (CH_2), 97.9, 98.6 ($CH^{pz,4}$), 124.9, 125.0 ($CH^{Ph,m}$), 127.5, 127.6 ($CH^{Ph,m}$), 129.8, 130.0 ($CH^{Ph,p}$), 139.9, 140.3, 140.6, 140.8, 142.3 ($C^{Ph,1/2/6}$), 154.1 ($C^{pz,3/5}$) ppm. IR (KBr): $\tilde{\nu}_{max.}$ = 3421 m, 3291 m, 3249 m, 2954 m, 2918 m, 2863 m, 1730 w, 1625 m, 1456 s, 1382 m, 1361 m, 1304 s, 1272 w, 1250 w, 1089 vs, 963 s, 925 s, 802 s, 759 m, 625 m, 519 m, 465 m cm^{-1}. M.p. > 240 °C. UV/Vis (CH_2Cl_2): λ (ε) = 353 nm (4387). MS (FAB): *m*/*z* (%) = 1103 (60) $[L^2_2Pd_2]^+$, 656 (60) $[L^2Pd_2]^+$. $C_{58}H_{82}B_2F_8N_8Pd_2$ (1277.78): calcd. C 54.54, H 6.42, N 8.77; found C 53.43, H 6.59, N 9.10.

Complex 7: Single crystals were obtained from acetonitrile/diethyl ether (yield of crystalline material 204 mg; 37%). The bulk crystalline material is a 2:1 mixture of compounds **7** and **3**, according to the ratio of the NMR signals observed for L^1 and L^2. ^{1}H NMR (300 MHz, $CDCl_3$): δ = 0.68 (s, 6 H, CH_3*iPr*), 0.87 (s, 6 H, CH_3*iPr*), 1.09, 1.12 (s, 12 H, CH_3 of L^1), 1.41, 1.48 (d, ^3J = 6 Hz, 6 H, CH_3*iPr*), 1.85 (m, 1 H, CH*iPr*), 2.18 (m, 6 H, CH_3*iPr*), 3.36−3.49 (m, CH_2), 3.95, 4.04 (s, 2 H, NH), 4.17, 4.20 (s, 12 H, CH_3 of L^1), 4.09−4.52 (m, CH_2), 4.90, 5.01 (s, 2 H, NH), 5.82 (s, 2 H, CH^{pz} of L^1), 5.92 (s, 1 H, CH^{pz} of L^2), 6.80−6.90 (m, CH^{Ar}), 7.10−7.23, 7.36−7.49 (m, CH^{Ar} and 1 H, CH*iPr*), 7.66 (d, ^3J = 7.4 Hz, 2 H, CH^{Ar}) ppm. ^{13}C NMR (300 MHz, $CDCl_3$): δ = 15.9, 16.6 (CH_3 of L^1), 22.0, 22.2, 22.7, 22.9, 25.6, 26.8 (CH_3 of L^1, L^2), 28.4 (CH*iPr*), 30.6 (CH*iPr*), 54.4, 54.6 (CH_2 of L^1), 55.3, 57.4 (CH_2 of L^2), 97.1 (CH^{pz} of L^1), 98.1 (CH^{pz} of L^2), 125.8, 128.3, 129.2, 129.4, 130.1, 130.3, 130.7, 131.8, 132.5, 132.9 (CH^{ar}), 138.5, 138.9, 142.1, 142.4 (C^{ar}), 157.5, 157.6 ($C^{pz,3/5}$) ppm. IR (KBr): $\tilde{\nu}_{max.}$ = 3225 m, 2952 m, 2931 m, 2860 w, 1622 w, 1524 w, 1461 s, 1443 s, 1382 s, 1361 m, 1307 s, 1253 w, 1094 vs, 961 w, 805 m, 777 m, 623 s, 570 w, 459 w, 418 w cm^{-1}. M.p.> 240 °C. UV/Vis (CH_3CN): λ (ε) = 218 (30808), 298 (9705), 499 (217). MS (FAB): *m*/*z* (%) = 995 (80) $[L^1L^2Ni_2ClO_4]^+$, 894 (100) $[L^1L^2Ni_2]^+$.

Table 1. Crystal data and refinement details for complexes **1**, **2**, **3**, **4**

	$[L^1_2Ni_2Cl_2]$ (**1**)	$[L^1_2Ni_2]Cl_2$ (**2**)	$[L^1_2Ni_2](ClO_4)_2$ (**3**)	$[L^1_2Pd_2](BF_4)_2$ (**4**)
Empirical formula	$C_{42}H_{50}Cl_2N_8Ni_2{\cdot}2[OC(CH_3)_2]$	$C_{42}H_{50}Cl_2N_8Ni_2{\cdot}4(CH_2Cl_2)$	$C_{42}H_{50}N_8O_8Cl_2Ni_2{\cdot}4(CH_3CN)$	$C_{42}H_{50}B_2F_8N_8Pd_2{\cdot}2(CH_2Cl_2, H_2O)$
M_r (g/mol)	971.35	1194.94	1147.39	1259.20
Crystal size (mm)	0.30 × 0.30 × 0.20	0.20 × 0.25 × 0.10	0.10 × 0.30 × 0.20	0.20 × 0.15 × 0.15
Crystal system	triclinic	monoclinic	triclinic	monoclinic
Space group	$P\bar{1}$	$C2/c$	$P\bar{1}$	$P2_1/c$
a (Å)	10.507(2)	32.664(7)	8.758(2)	13.909(3)
b (Å)	13.559(3)	13.841(3)	11.006(2)	10.012(2)
c (Å)	17.019(3)	11.991(2)	15.009(3)	19.084(4)
α (deg)	81.55(3)	90	107.32(3)	90
β (deg)	77.14(3)	103.00(3)	98.62(3)	108.71(3)
γ (deg)	88.63(3)	90	103.85(3)	90
Volume (Å^3)	2338.0	5282.3	1302.3	2517.2
Z	2	4	1	2
$\rho_{calcd.}$ (g/cm^3)	1.363	1.503	1.463	1.661
F(000)	1024	2464	600	1272
hkl range	−12−13, ±16, ±21	±42, ±17, ±15	±11, ±14, ±19	±18, ±12, −25−27
Temperature (K)	200	200	200	200
2θ range	$3.6 < 2\theta < 52.4$	$2.6 < 2\theta < 55$	$4.1 < 2\theta < 55.1$	$3.1 < 2\theta < 60.8$
Measured reflections	37920	44628	11835	11548
Unique reflections	9226	6057	5991	5793
Obsd. reflections $[I > 2\sigma(I)]$	5172	4382	4617	4900
Refined parameters	592	414	345	407
Residual electron density (e·Å^{-3})	0.55	0.60	0.67	1.66
$R1$ $[I > 2\sigma(I)]$	0.042	0.039	0.039	0.036
$wR2$ (all data)	0.105	0.096	0.099	0.094
Goodness-of-fit	0.966	0.997	1.071	1.080

Table 2. Crystal data and refinement details for complexes **5**, **6**, **7** and **8**

	$[L^2_2 Ni_2](ClO_4)_2$ (**5**)	$[L^2_2Pd_2](BF_4)_2$ (**6**)	$[L^1L^2Ni_2](ClO_4)_2$ (**7**)	$[L^3_2Ni_2](ClO_4)_2$ (**8**)
Formula	$C_{58}H_{82}N_8O_8Cl_2Ni_2{\cdot}1.4$ $[OC(CH_3)_2]$ 0.4 C_2H_5OH	$C_{58}H_{82}B_2F_8N_8Pd_2{\cdot}2$ (CH_2Cl_2)	$C_{50}H_{66}Cl_2N_8Ni_2O_8{\cdot}1.5$ (CH_3CN)	$C_{46}H_{58}Cl_2N_8Ni_2O_8{\cdot}2$ (C_2H_5CN)
M_r (g/mol)	1307.35	1447.59	1157.01	1149.48
Crystal size (mm)	0.08 × 0.20 × 0.30	0.06 × 0.23 × 0.38	0.10 × 0.10 × 0.05	0.35 × 0.26 × 0.24
Crystal system	triclinic	triclinic	orthorhombic	triclinic
Space group	$P\bar{1}$	$P\bar{1}$	$Pbca$	$P\bar{1}$
a (Å)	10.760(2)	11.4267(5)	17.380(4)	9.2380(1)
b (Å)	11.073(2)	12.3828(6)	18.230(4)	9.2919(1)
c (Å)	15.022(3)	13.4776(6)	35.150(7)	16.3793(3)
α (deg)	106.21(3)	80.048(3)	90	99.750(1)
β (deg)	96.44(3)	66.255(3)	90	96.833(1)
γ (deg)	101.36(3)	69.194(3)	90	98.877(1)
Volume (Å^3)	1658.2	1630.75	11137.0	1353.78(3)
Z	1	1	8	1
$\rho_{calcd.}$ (g/cm^3)	1.309	1.474	1.380	1.410
F(000)	697	744	4872	604
hkl range	±42, ±17, ±15	−13−15, ±16, 0−17	±23, ±25, ±49	−12−11, ±12. 0−21
Temperature (K)	200	173	200	173
2θ range	$3.9 < 2\theta < 52.0$	$3.3 < 2\theta < 56.8$	$3.4 < 2\theta < 60.3$	$4.52 < 2\theta < 56.64$
Measured reflections	11777	22195	29886	18243
Unique reflections	6132	8020	15258	6599
Obsd. reflections $[I > 2\sigma(I)]$	4487	6181	6187	5830
Refined parameters	392	541	735	468
Residual electron density (e·Å^{-3})	0.93	1.95	0.69	0.54
$R1$ $[I > 2\sigma(I)]$	0.052	0.054	0.079	0.032
$wR2$ (all data)	0.144	0.156	0.227	0.092
Goodness-of-fit	1.048	1.043	0.966	1.059

Complex 8: Single crystals were obtained from acetonitrile/diethyl ether (yield of crystalline material 105 mg; 20%). ^{1}H NMR (300 MHz, $CDCl_3$, 333 K): δ = 1.03 (br. s, CH_3), 2.80 (br. s, CH*iPr*), 6.69 ($CH^{pz,4}$), 7.67, 7.96, 8.50 (br. s, CH^{Ph}) ppm, CH_2 not observed. ^{13}C NMR (300 MHz, $CDCl_3$): no signals observed. IR (KBr): $\tilde{\nu}_{max.}$ = 3425 w, 3226 s, 2935 s, 2921 m, 2879 w, 1484 s, 1437 m, 1383 m, 1359 w, 1312 s, 1237 w, 1112 vs, 1102 vs, 1088 vs, 1030 vs, 944 w, 929 w, 91 w, 763 s, 622 vs, 526 m, 461 w, 420 w cm^{-1}. M.p.> 240 °C. UV/Vis (CH_3CN): λ (ε) = 216 (28006), 242 (20310), 285 (7708), 477 (361). MS (FD): *m*/*z* (%) = 939 (100) $[L_2^3Ni_2(ClO_4)]^+$, 839 (10) $[L_2^3Ni_2]^+$. $C_{46}H_{58}Cl_2N_8Ni_2O_8$ (1039.29): calcd. C 53.16, H 5.63, N 10.78; found C 53.00, H 5.57, N 10.80.

X-ray Crystallographic Studies: The measurements for **1**, **2**, **3**, **4**, **5** and **7** were carried out with a Nonius Kappa CCD diffractometer and for **6** and **8** with a Bruker-AXS-CCD diffractometer, using graphite-monochromated Mo-K_α radiation. All calculations were performed using the SHELXT PLUS software package.[52] Structures were solved by direct methods with SHELXS-97 and refined with SHELXL-97. Atomic coordinates and thermal parameters of the non-hydrogen atoms were refined in fully or partially anisotropic models by full-matrix least-squares calculation based on F^2. In general the hydrogen atoms were placed in calculated positions and allowed to ride on the atoms to which they are attached. Table 1 and Table 2 shows a compilation of the data for the structure determinations.

CCDC-222584 (for **1**), -222585 (for **2**), -222586 (for **3**), -222587 (for **4**), -222588 (for **5**), -222589 (for **6**), -222590 (for **7**) and -222591 (for **8**) contain the supplementary crystallographic data for this paper. These data can be obtained free of charge at www.ccdc.cam.ac.uk/conts/retrieving.html [or from the Cambridge Crystallographic Data Center, 12 Union Road, Cambridge CB2 1EZ, UK; Fax: (internat.) +44-1223-336-033; E-mail: deposit@ccdc.cam.ac.uk].

Acknowledgments

F. M. sincerely thanks Prof. Dr. G. Huttner for his generous support and Dr. S. Dechert for valuable discussions. Funding from the DFG (SFB, 247, Graduiertenkolleg-Fellowship to J. C. R.) and the Fonds der Chemischen Industrie (F. M.) is gratefully acknowledged.

[1] K. D. Karlin, *Science* **1993**, *261*, 701−708.
[2] E. K. van den Beuken, B. L. Feringa, *Tetrahedron* **1998**, *54*, 12985−13011.
[3] H. Steinhagen, G. Helmchen, *Angew. Chem.* **1996**, *108*, 2489−2492; *Angew. Chem. Int. Ed. Engl.* **1996**, *35*, 2339−2342.
[4] O. Kahn, *Molecular Magnetism*, Wiley-VCH, Weinheim, **1993**.
[5] S. Trofimenko, *Progr. Inorg. Chem.* **1986**, *34*, 115−210.
[6] G. La Monica, G. A. Ardizzoia, *Progr. Inorg. Chem.* **1997**, *46*, 151−238.
[7] F. Meyer, S. Beyreuther, K. Heinze, L. Zsolnai, *Chem. Ber./Recl.* **1997**, *130*, 605−613.
[8] F. Meyer, P. Rutsch, *Chem. Commun.* **1998**, 1037−1038.
[9] T. Kamiusuki, H. Okawa, N. Matsumoto, S. Kida, *J. Chem. Soc., Dalton Trans.* **1990**, 195−198.
[10] C. W. Hahn, P. G. Rasmussen, J. Carlos Bayón, *Inorg. Chem.* **1992**, *31*, 1963−1965.
[11] J. Pons, X. López, J. Casabó, F. Teixidor, A. Caubet, J. Rius, C. Miravitlles, *Inorg. Chim. Acta* **1992**, *195*, 61−66.
[12] B. Mernari, F. Abraham, M. Lagrenee, M. Drillon, P. Legoll, *J. Chem. Soc., Dalton Trans.* **1993**, 1707−1711.
[13] F. Meyer, A. Jacobi, L. Zsolnai, *Chem. Ber./Recl.* **1997**, *130*, 1441−1447.
[14] M. Itoh, K.-I. Motoda, K. Shindo, T. Kamiusuki, H. Sakiyama, N. Matsumoto, H. Okawa, *J. Chem. Soc., Dalton Trans.* **1995**, 3635−3641.
[15] F. Escartí, C. Miranda, L. Lamarque, J. Latorre, E. García-España, M. Kumar, V. J. Arán, P. Navarro, *Chem. Commun.* **2002**, 936−937.
[16] T. G. Schenck, C. R. C. Milne, J. F. Sawyer, B. Bosnich, *Inorg. Chem.* **1985**, *24*, 2338−2344.
[17] T. Kamiusuki, H. Okawa, E. Kitaura, M. Koikawa, N. Matsumoto, S. Kida, H. Oshio, *J. Chem. Soc., Dalton Trans.* **1989**, 2077−2081.
[18] T. A. Kaden, *Coord. Chem. Rev.* **1999**, *190−192*, 371−389.
[19] J.-L. Chou, D.-N. Horng, J.-P. Chyn, K.-M. Lee, F. L. Urbach, G.-H. Lee, H.-L. Tsai, *Inorg. Chem. Commun.* **1999**, *2*, 392−395.
[20] S. Tanaka, M. Akita, *Angew. Chem.* **2001**, *113*, 2951−2953; *Angew. Chem. Int. Ed.* **2001**, *40*, 2865−2867.
[21] F. Meyer, K. Heinze, B. Nuber, L. Zsolnai, *J. Chem. Soc., Dalton Trans.* **1998**, 207−214.
[22] F. Meyer, E. Kaifer, P. Kircher, K. Heinze, H. Pritzkow, *Chem. Eur. J.* **1999**, *5*, 1617−1630.
[23] F. Meyer, I. Hyla-Kryspin, E. Kaifer, P. Kircher, *Eur. J. Inorg. Chem.* **2000**, 771−781.
[24] S. Buchler, F. Meyer, E. Kaifer, H. Pritzkow, *Inorg. Chim. Acta* **2002**, *337*, 371−386.
[25] J. C. Röder, F. Meyer, H. Pritzkow, *Chem. Commun.* **2001**, 2176−2177.
[26] J. C. Röder, G. Noel, F. Meyer, unpublished results.
[27] J. C. Röder, F. Meyer, M. Konrad, S. Sandhöfner, E. Kaifer, H. Pritzkow, *Eur. J. Org. Chem.* **2001**, 4479−4487.
[28] The angular structural parameter τ is defined as τ = (β − α)/60, where α and β represent two basal angles with β > α. It is a measure of the degree of trigonality: a perfect TB-5 structure is associated with τ = 1, while τ = 0 is expected for an idealized SPY-5 geometry: A. W. Addison, T. N. Rao, J. Reedijk, J. van Rijn, G. C. Verschoor, *J. Chem. Soc., Dalton Trans.* **1984**, 1349−1356.
[29] C. Janiak, *J. Chem. Soc., Dalton Trans.* **2000**, 3885−3896.
[30] C. J. O′Connor, *Inorg. Chem.* **1982**, *29*, 203−283.
[31] N_α refers to the temperature-independent paramagnetism [100 × 10^{-6} cm^3/mol per nickel(II) ion[29]]; all other parameters have their usual meaning. $\chi_{dim} = (Ng^2\mu_B{}^2/kT)\cdot[2\exp(2J/kT) + 10\exp(6J/kT)]/[1 + 3\exp(2J/kT) + 5\exp(6J/kT)]$; $\chi_{mono} = 2Ng^2\mu_B{}^2/3kT$; $R = \Sigma(\chi^{calcd.} - \chi^{obsd.})^2/\Sigma(\chi^{obsd.})^2$.
[32] P. Chaudhuri, H.-J. Küppers, K. Wieghardt, S. Gehring, W. Haase, B. Nuber, J. Weiss, *J. Chem. Soc., Dalton Trans.* **1988**, 1367−1370.
[33] L. Siegfried, T. A. Kaden, F. Meyer, P. Kircher, H. Pritzkow, *J. Chem. Soc., Dalton Trans.* **2001**, 2310−2315.
[34] J. Casabó, J. Pons, K. S. Siddiqi, F. Teixidor, E. Molins, C. Miravitlles, *J. Chem. Soc., Dalton Trans.* **1989**, 1401−1403.
[35] J. Pons, X. López, E. Benet, J. Casabó, *Polyhedron* **1990**, *9*, 2839−2845.
[36] V. P. Hanot, T. D. Robert, J. Kolnaar, J. G. Haasnoot, J. Reedijk, H. Kooijman, A. L. Spek, *J. Chem. Soc., Dalton Trans.* **1996**, 4275−4281.
[37] C. J. Ballhausen, A. D. Liehr, *J. Am. Chem. Soc.* **1959**, *81*, 538−542.
[38] L. Brammer, *Dalton Trans.* **2003**, 3145−3157.
[39] M. Brookhart, M. L. H. Green, *J. Organomet. Chem.* **1983**, *250*, 395−408.
[40] R. H. Crabtree, *Angew. Chem.* **1993**, *105*, 828−845; *Angew. Chem. Int. Ed. Engl.* **1993**, *32*, 789−806.
[41] D. Braga, F. Grepioni, E. Tedesco, K. Biradha, G. R. Desiraju, *Organometallics* **1997**, *16*, 1846−1856.
[42] A. Martín, *J. Chem. Ed.* **1999**, *76*, 578−583.
[43] J. Y. Saillard, R. Hoffman, *J. Am. Chem. Soc.* **1984**, *106*, 2006−2026.

[44] A. Albinati, C. G. Anklin, F. Ganazzoli, H. Rüegg, P. S. Pregosin, *Inorg. Chem.* **1987**, *26*, 50−508.
[45] A. Albinati, C. Arz, P. S. Pregosin, *Inorg. Chem.* **1987**, *26*, 508−513.
[46] A. Albinati, P. S. Pregosin, F. Wombacher, *Inorg. Chem.* **1990**, *29*, 1812−1817.
[47] M. Bortolin, U. E. Bucher, H. Rüegger, L. M. Venanzi, A. Albinati, F. Lianza, S. Trofimenko, *Organometallics* **1992**, *11*, 2514−2521.
[48] I. C. M. Wehman-OoYevaar, D. M. Grove, H. Kooijman, P. van der Sluis, A. L. Spek, G. Van Koten, *J. Am. Chem. Soc.* **1992**, *114*, 9916−9924.
[49] J. M. Casas, L. R. Falvello, J. Fourníes, A. Martín, A. J. Welch, *Inorg. Chem.* **1996**, *35*, 6009−6014.
[50] T. Kawamoto, I. Nagasawa, H. Kuma, Y. Kushi, *Inorg. Chem.* **1996**, *35*, 2427−2432.
[51] T. W. Hambley, *Inorg. Chem.* **1998**, *37*, 3767−3774.
[52] G. M. Sheldrick, *SHELXL-97, Program for Crystal Structure Refinement*, University of Göttingen, **1997**; G. M. Sheldrick, *SHELXS-97, Program for Crystal Structure Solution*, University of Göttingen, **1997**.

Received October 23, 2003
Early View Article
Published Online March 9, 2004

